Application of the Hydroelastic Theory of Ships to the Motion of Ice Shelves

M. H. Meylan[1], L. G. Bennetts[2], M. Ilyas[1], B. Lamichhane[1] and M. A. Peter[3]

[1]School of Mathematical and Physical Sciences, University of Newcastle, Australia
[2]School of Mathematical Sciences, University of Adelaide, Adelaide, SA 5005, Australia.
[3]Institute of Mathematics, University of Augsburg, 86135 Augsburg, Germany
e-mail address: mike.meylan@newcastle.edu.au

HIGHLIGHTS

We show that the methods used to analyse complex hydroelastic behaviour of ships can be applied to model the motion of ice shelves. We use a special boundary condition and the finite element method, which is suited to extension to complex geometries, to solve Laplace's equation. We present example calculations in the time–domain that show the importance of resonances.

1 Introduction and Problem Formulation

We are interested in modelling the impact of very long ocean surface waves on ice shelves, primarily waves in the tsunami–infragravity regime (Cathles *et al.*, 2009; Bromirski *et al.*, 2015, 2017), using methods developed to predict the hydroelastic motion of ships. We calculate the time-dependent response of an ice shelf to wave forcing using the frequency-domain solution. The boundary conditions at the front of the ice shelf, coupling it to the surrounding fluid, are written as a special non-local linear operator with forcing. The ice shelf motion is expanded using the in vacuo elastic modes and the method of added mass and damping, commonly used in the hydroelasticity of ships, is employed. The analysis is extended from the frequency domain to the time domain, and the resonant behaviour of the system is studied.

Time-dependent water motions are described by the velocity potential $\Phi(\mathbf{x}, t)$, which is governed by the linearized water-wave equations. The fluid is of constant depth h and the ice shelf extends from $x = -L$ to $x = 0$. We assume that the ice shelf can be modelled as a thin plate of uniform thickness. We introduce non-dimensional equations by scaling the length with respect to the water depth (which becomes unity) and time with respect to $\sqrt{h/g}$. The non-dimensional equations and coordinate system are shown in the schematic diagram below.

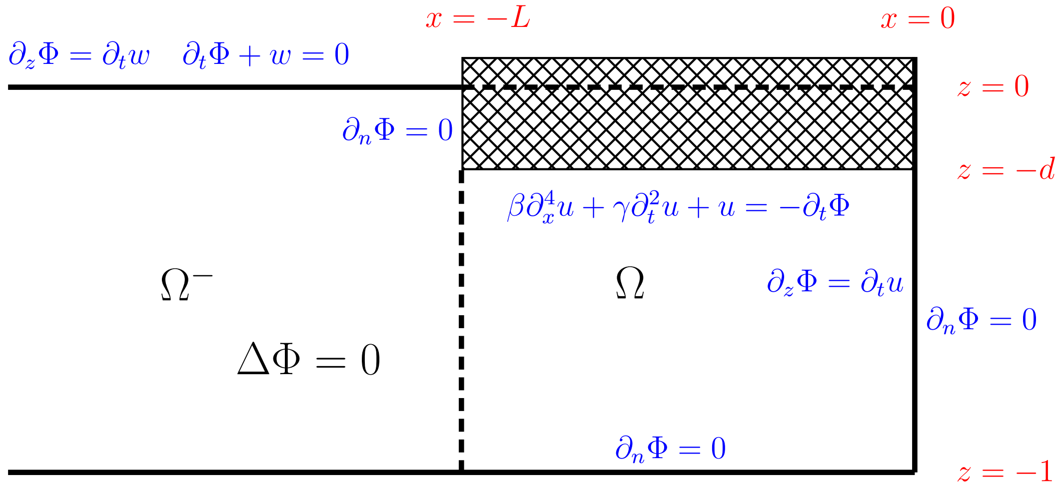

2 Solution of the frequency-domain equations

To convert to the frequency domain we simply assume that all quantities are proportional to $\exp(-\mathrm{i}\omega t)$, and write

$$w(x,t) = \mathrm{Re}\left\{\zeta(x)\mathrm{e}^{-\mathrm{i}\omega t}\right\}, \quad u(x,t) = \mathrm{Re}\left\{\eta(x)\mathrm{e}^{-\mathrm{i}\omega t}\right\},$$

$$\text{and} \quad \Phi(x,z,t) = \mathrm{Re}\left\{\phi(x,z)\mathrm{e}^{-\mathrm{i}\omega t}\right\},$$

The potential in the semi-infinite open water region Ω^- is

$$\phi(x,z) = \frac{\cosh K(z+1)}{\cosh K}\mathrm{e}^{\mathrm{i}Kx} + \sum_{p=0}^{\infty} c_p \tau_{p,0}(z)\,\mathrm{e}^{k_{p,0}(x+L)}, \tag{1}$$

where the first term on the right-hand side represents the unit-amplitude (in potential) incident wave, with the wavenumber K being the positive real solution of the dispersion relation

$$K \tanh K = \alpha.$$

The functions $\tau_{p,0}(z)$ are orthonormal modes given by

$$\tau_{p,0}(z) = N_{p,0}^{-1}\cos k_{p,0}(z+1) \quad \text{where} \quad N_{p,0} = \sqrt{\frac{1}{2} + \frac{\sin(2k_{p,0})}{4k_{p,0}}},$$

and the wavenumbers $k_{p,0}$ are solutions of the dispersion relation

$$k_{p,0}\tan k_{p,0} = -\alpha,$$

with $k_{0,0} = -\mathrm{i}K$ defining the wave reflected by the shelf, $k_{1,0} < k_{2,0} < \cdots \in \mathbb{R}^+$ defining evanescent waves that decay away from the shelf, and c_p are as yet unknown amplitudes.

We are going to solve for the motion in the sub-ice shelf cavity, Ω, using the finite element method, requiring a boundary condition at $x = 0$. At the interface between the open water and the shelf/cavity regions, $x = -L^+$ (i.e. the limit from the ice shelf covered region), the potential and the normal derivative are expanded as follows

$$\phi\left(-L^+, z\right) = \sum_{p=0}^{N} a_p \tau_{p,d}(z), \quad -1 < z < -d,$$

$$\partial_x \phi\left(-L^+, z\right) = \sum_{p=0}^{N} b_p \tau_{p,d}(z), -1 < z < -d.$$

The functions $\tau_{p,d}(z)$ are orthonormal modes given by

$$\tau_{p,d}(z) = N_{p,d}^{-1}\cos k_{p,d}(z+1) \quad \text{where} \quad N_{p,d} = \sqrt{\frac{1-d}{2} + \frac{\sin(2k_{p,d}(1-d))}{4k_{p,d}}},$$

in which $k_{p,d}\,(p \geq 1)$ are positive real solutions and $k_{0,d}$ is the negative imaginary solution of the dispersion equation

$$-k_{p,d}\tan(k_{p,d}(1-d)) = \alpha.$$

We require a mapping from the coefficients a_p to b_p. We find this by matching this potential and its derivative with the solution in the open water Ω^-.

We derive two equations at $x = -L$. The first comes from matching the potential and taking the inner product with respect to $\tau_{q,d}(z)$ for $q = 0, 1, \dots$

$$\int_{-1}^{-d} \frac{\cosh K(z+1)}{\cosh K} \mathrm{e}^{-\mathrm{i}KL} \tau_{q,d}(z)\ \mathrm{d}z + \sum_{p=0}^{N} c_p \int_{-1}^{-d} \tau_{p,0}(z)\, \tau_{q,d}(z)\ \mathrm{d}z = a_q,$$

or in the matrix form

$$\mathbf{f} + \mathbf{M}\mathbf{c} = \mathbf{a}. \tag{2}$$

Similarly, taking the inner product of the matching of the normal with respect to $\tau_{q,0}(z)$ for $q = 0, 1, \dots,$ we obtain

$$-\int_{-1}^{0} \mathrm{i}K \frac{\cosh K(z+1)}{\cosh K} \mathrm{e}^{-\mathrm{i}KL} \tau_{q,0}(z)\ \mathrm{d}z - k_q c_q = \sum_{p=0}^{N} b_p \int_{-1}^{-d} \tau_{p,d}(z)\, \tau_{q,0}(z)\ \mathrm{d}z,$$

or in matrix form

$$-\mathbf{g} - \lceil k \rfloor \mathbf{c} = \mathbf{M}^T \mathbf{b}. \tag{3}$$

Systems (2) and (3) can be combined to eliminate the unknown amplitudes in the open water, $\mathbf{c}$, leaving the condition

$$\mathbf{b} = -\left(\mathbf{M} \lceil k \rfloor^{-1} \mathbf{M}^T\right)^{-1} \mathbf{a} - \left(\mathbf{M} \lceil k \rfloor^{-1} \mathbf{M}^T\right)^{-1} \left(\mathbf{M} \lceil k \rfloor^{-1} \mathbf{g} - \mathbf{f}\right).$$

This provides the necessary mapping between the expansion of the potential and its horizontal derivative at $x = -L$, and is the Dirichlet–to–Neumann map in our expansion a_p for the potential and b_p for the normal derivative. The solution of Laplace's equations beneath the ice shelf are found using the finite element method.

The frequency-domain version of the boundary condition beneath the ice shelf is

$$\beta \partial_x^4 \eta - \gamma \omega^2 \eta + \eta = \mathrm{i}\omega\phi, \tag{4}$$

with boundary conditions $\partial_x^2 \eta = \partial_x^3 \eta = 0,\ \ x = -L,$ and $\eta = \partial_x \eta = 0,\ \ x = 0$. We expand the ice shelf motion using its in vacuo modes

$$\eta(x) = \sum_{j=1}^{\infty} \lambda_j \eta^j(x), \tag{5}$$

where λ_j are coefficients that are to be determined. The modes satisfy the ordinary differential equation

$$\frac{d^4}{dx^4} \eta^j(x) - \mu_j^4 \eta^j(x) = 0, \tag{6}$$

and the boundary conditions.

The corresponding expansion of the velocity potential in the cavity, Ω, is

$$\phi(x,z) = \phi^0(x,z) + \sum_{j=1}^{\infty} \lambda_j \phi^j(x,z), \tag{7}$$

where ϕ^0 is the diffraction potential and ϕ^j $(j = 1, 2, \dots)$, are the radiation potentials found using the finite element method. In the standard way we can then write the solution as

$$\left(\mathbf{K} - \omega^2 \mathbf{M} + \mathbf{C} + \omega^2 \mathbf{A} - \mathrm{i}\omega \mathbf{B}\right) \boldsymbol{\lambda} = \frac{\mathrm{i}\alpha}{\omega} \mathbf{f}, \tag{8}$$

where the matrices are known as the stiffness, mass, restoring force, added mass and damping.

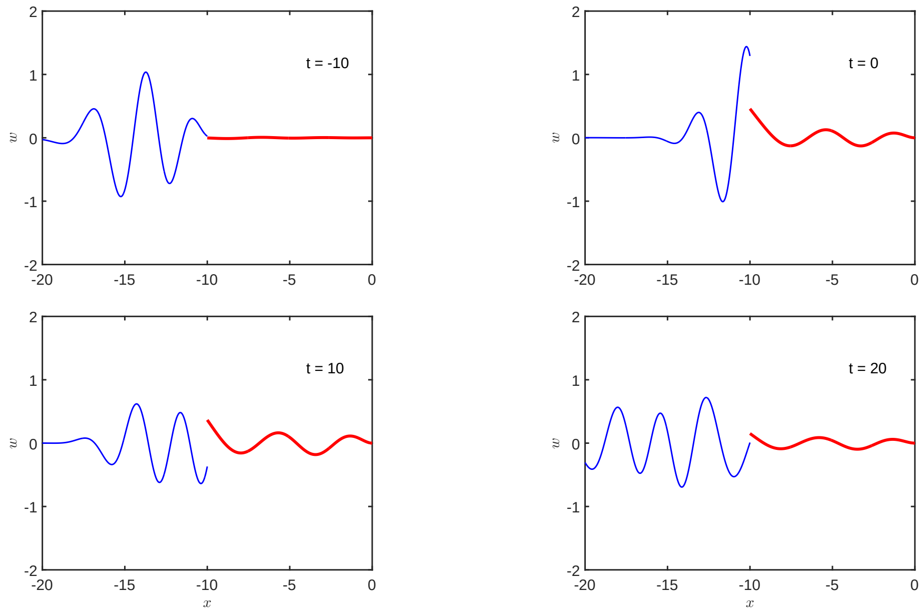

Figure 1: The displacement for the free surface (blue) and the plate (red) for a Gaussian input given by $\hat{f}(K) = \frac{2}{\pi}\mathrm{e}^{-2(K-2)^2}\mathrm{e}^{\mathrm{i}LK}$.

3 Time-domain solution and Numerical Results.

The time-domain solution for the free-surface potential is given by

$$\zeta(x,t) = \mathrm{Re}\left\{\frac{1}{\pi}\int_0^\infty \hat{f}(K)\zeta(x:\omega(K))\mathrm{e}^{-\mathrm{i}\omega t}\,\mathrm{d}K\right\}, \tag{9}$$

where $\hat{f}(K)$ of the incident wave packet. The displacement of the plate is given analogously.

Figure 1 shows the solution for 6 instants of time. The excitation of the four node mode is visible, as expected since this is the mode response which is closest to our centre frequency. Further numerical solutions will be presented at the workshop.

4 Conclusions

We have shown here how the motion of an ice shelf to wave forcing can be computed using methods developed to analyse the hydroelastic behaviour of ships. We have also shown that this method allows us to compute the motion in the time domain and to understand the resonant response. The finite element method was used to model the fluid as it is ideally suited for extensions to more complex, and realistic cavity shapes, and to the computation of the elastic response for shelves of complex geometry. Such computations would greatly aid our understanding of ice shelf vibration.

Acknowledgments

This material is based upon research supported in part by ONR (N0001415-12611 (MHM)), the Isaac Newton Institute (EP/K032208/1, (MHM and LGB)) and the Simons Foundation (MHM and LGB).

References

Bromirski, Peter D, Chen, Zhao, Stephen, Ralph A, Gerstoft, Peter, Arcas, D, Diez, Anja, Aster, Richard C, Wiens, Douglas A & Nyblade, Andrew 2017 Tsunami and infragravity waves impacting antarctic ice shelves. *Journal of Geophysical Research: Oceans* .

Bromirski, Peter D., Diez, A., Gerstoft, P., Stephen, Ralph A., Bolmer, T., Wiens, D. A., Aster, R. & Nyblade, N. 2015 Ross ice shelf vibrations. *Geophys. Res. Lett.* **42**, 7589–7597.

Cathles, LM, Okal, Emile A & MacAyeal, Douglas R 2009 Seismic observations of sea swell on the floating ross ice shelf, antarctica. *Journal of Geophysical Research: Earth Surface* **114** (F2).